Belle Preprint 2005-18
KEK Preprint 2005-15

Measurement of $|V_{ub}|$ near the endpoint of the electron momentum spectrum from semileptonic B-meson decays

Belle Collaboration

A. Limosani [g], K. Abe [g], K. Abe [am], I. Adachi [g], H. Aihara [ao], Y. Asano [as], T. Aushev [k], S. Bahinipati [d], A. M. Bakich [aj], E. Barberio [s], U. Bitenc [ℓ], I. Bizjak [ℓ], S. Blyth [x], A. Bondar [a], A. Bozek [y], M. Bračko [g,r,ℓ], J. Brodzicka [y], T. E. Browder [f], Y. Chao [x], A. Chen [v], K.-F. Chen [x], W. T. Chen [v], B. G. Cheon [c], R. Chistov [k], Y. Choi [ai], A. Chuvikov [af], S. Cole [aj], J. Dalseno [s], M. Danilov [k], M. Dash [at], J. Dragic [g], A. Drutskoy [d], S. Eidelman [a], S. Fratina [ℓ], N. Gabyshev [a], T. Gershon [g], G. Gokhroo [ak], B. Golob [q,ℓ], A. Gorišek [ℓ], T. Hara [ac], N. C. Hastings [ao], K. Hayasaka [t], H. Hayashii [u], M. Hazumi [g], L. Hinz [p], T. Hokuue [t], Y. Hoshi [am], S. Hou [v], W.-S. Hou [x], T. Iijima [t], A. Imoto [u], K. Inami [t], A. Ishikawa [g], R. Itoh [g], M. Iwasaki [ao], Y. Iwasaki [g], J. H. Kang [au], J. S. Kang [n], N. Katayama [g], H. Kawai [b], T. Kawasaki [aa], H. R. Khan [ap], H. Kichimi [g], H. J. Kim [o], H. O. Kim [ai], S. K. Kim [ah], S. M. Kim [ai], K. Kinoshita [d], S. Korpar [r,ℓ], P. Krokovny [a], R. Kulasiri [d], S. Kumar [ad], C. C. Kuo [v], Y.-J. Kwon [au], J. S. Lange [e], G. Leder [j], T. Lesiak [y], J. Li [ag], S.-W. Lin [x], D. Liventsev [k], J. MacNaughton [j], G. Majumder [ak], F. Mandl [j], T. Matsumoto [aq], Y. Mikami [an], W. Mitaroff [j], K. Miyabayashi [u], H. Miyake [ac], H. Miyata [aa], R. Mizuk [k], D. Mohapatra [at], T. Mori [ap], T. Nagamine [an], Y. Nagasaka [h], E. Nakano [ab], M. Nakao [g], Z. Natkaniec [y], S. Nishida [g],

O. Nitoh [ar], T. Nozaki [g], S. Ogawa [aℓ], T. Ohshima [t], T. Okabe [t], S. Okuno [m], S. L. Olsen [f], Y. Onuki [aa], W. Ostrowicz [y], H. Ozaki [g], H. Palka [y], C. W. Park [ai], H. Park [o], N. Parslow [aj], R. Pestotnik [ℓ], L. E. Piilonen [at], F. J. Ronga [g], H. Sagawa [g], Y. Sakai [g], N. Sato [t], T. Schietinger [p], O. Schneider [p], C. Schwanda [j], R. Seuster [f], M. E. Sevior [s], H. Shibuya [aℓ], B. Shwartz [a], V. Sidorov [a], A. Somov [d], R. Stamen [g], S. Stanič [as,1], M. Starič [ℓ], K. Sumisawa [ac], T. Sumiyoshi [aq], S. Y. Suzuki [g], O. Tajima [g], F. Takasaki [g], K. Tamai [g], N. Tamura [aa], M. Tanaka [g], Y. Teramoto [ab], X. C. Tian [ae], T. Tsukamoto [g], S. Uehara [g], K. Ueno [x], T. Uglov [k], S. Uno [g], P. Urquijo [s], G. Varner [f], K. E. Varvell [aj], S. Villa [p], C. C. Wang [x], C. H. Wang [w], M.-Z. Wang [x], Q. L. Xie [i], B. D. Yabsley [at], A. Yamaguchi [an], H. Yamamoto [an], Y. Yamashita [z], M. Yamauchi [g], J. Ying [ae], J. Zhang [g], L. M. Zhang [ag], Z. P. Zhang [ag], and D. Žontar [q,ℓ]

[a] *Budker Institute of Nuclear Physics, Novosibirsk, Russia*

[b] *Chiba University, Chiba, Japan*

[c] *Chonnam National University, Kwangju, South Korea*

[d] *University of Cincinnati, Cincinnati, OH, USA*

[e] *University of Frankfurt, Frankfurt, Germany*

[f] *University of Hawaii, Honolulu, HI, USA*

[g] *High Energy Accelerator Research Organization (KEK), Tsukuba, Japan*

[h] *Hiroshima Institute of Technology, Hiroshima, Japan*

[i] *Institute of High Energy Physics, Chinese Academy of Sciences, Beijing, PR China*

[j] *Institute of High Energy Physics, Vienna, Austria*

[k] *Institute for Theoretical and Experimental Physics, Moscow, Russia*

[ℓ] *J. Stefan Institute, Ljubljana, Slovenia*

[m] *Kanagawa University, Yokohama, Japan*

[n] *Korea University, Seoul, South Korea*

[o] *Kyungpook National University, Taegu, South Korea*

[p] *Swiss Federal Institute of Technology of Lausanne, EPFL, Lausanne, Switzerland*

[q] *University of Ljubljana, Ljubljana, Slovenia*

[r] *University of Maribor, Maribor, Slovenia*

[s] *University of Melbourne, Victoria, Australia*

[t] *Nagoya University, Nagoya, Japan*
[u] *Nara Women's University, Nara, Japan*
[v] *National Central University, Chung-li, Taiwan*
[w] *National United University, Miao Li, Taiwan*
[x] *Department of Physics, National Taiwan University, Taipei, Taiwan*
[y] *H. Niewodniczanski Institute of Nuclear Physics, Krakow, Poland*
[z] *Nihon Dental College, Niigata, Japan*
[aa] *Niigata University, Niigata, Japan*
[ab] *Osaka City University, Osaka, Japan*
[ac] *Osaka University, Osaka, Japan*
[ad] *Panjab University, Chandigarh, India*
[ae] *Peking University, Beijing, PR China*
[af] *Princeton University, Princeton, NJ, USA*
[ag] *University of Science and Technology of China, Hefei, PR China*
[ah] *Seoul National University, Seoul, South Korea*
[ai] *Sungkyunkwan University, Suwon, South Korea*
[aj] *University of Sydney, Sydney, NSW, Australia*
[ak] *Tata Institute of Fundamental Research, Bombay, India*
[aℓ] *Toho University, Funabashi, Japan*
[am] *Tohoku Gakuin University, Tagajo, Japan*
[an] *Tohoku University, Sendai, Japan*
[ao] *Department of Physics, University of Tokyo, Tokyo, Japan*
[ap] *Tokyo Institute of Technology, Tokyo, Japan*
[aq] *Tokyo Metropolitan University, Tokyo, Japan*
[ar] *Tokyo University of Agriculture and Technology, Tokyo, Japan*
[as] *University of Tsukuba, Tsukuba, Japan*
[at] *Virginia Polytechnic Institute and State University, Blacksburg, VA, USA*
[au] *Yonsei University, Seoul, South Korea*

Abstract

We report measurements of partial branching fractions of inclusive charmless semileptonic B-meson decays at the endpoint of the electron momentum spectrum. The measurements are made in six overlapping momentum intervals that have lower bounds ranging from 1.9 GeV/c to 2.4 GeV/c and a common upper bound of 2.6 GeV/c, as measured in the centre of mass frame. The results are based on a sample of 29 million $B\overline{B}$ pairs, accumulated by the Belle detector at the KEKB asymmetric e^+e^- collider operating on the $\Upsilon(4S)$ resonance. In the momentum

interval ranging from 1.9 GeV/c to 2.6 GeV/c we measure the partial branching fraction $\Delta\mathcal{B}(B \to X_u e\nu_e) = (8.47 \pm 0.37 \pm 1.53) \times 10^{-4}$, where the first error is statistical and the second is systematic. A prediction of the partial rate $R = (21.69 \pm 3.62^{+2.18}_{-1.98})\,|V_{ub}|^2\mathrm{ps}^{-1}$ in this momentum interval based on theory is calculated with input HQET parameters that have been derived from Belle's measurement of the $B \to X_s\gamma$ photon energy spectrum, where the first error is due to the uncertainty on HQET parameters and the second error is from theory. Using both $\Delta\mathcal{B}(B \to X_u e\nu_e)$ and R we find $|V_{ub}| = (5.08 \pm 0.47 \pm 0.42^{+0.26}_{-0.23}) \times 10^{-3}$, where the first error is from the partial branching fraction, and the second and third errors are from uncertainties in R.

Key words: Semileptonic B-meson decays; CKM matrix
PACS: 11.30.Er, 13.20.He, 12.15.Ff, 14.40.Nd

1 Introduction

The magnitude of the Cabibbo-Kobayashi-Maskawa (CKM) matrix element $|V_{ub}|$ is a fundamental parameter of the Standard Model (SM). A knowledge of its value is crucial to the understanding of CP violation within the SM, which is underpinned by knowledge of the so-called Unitarity Triangle (UT). Recent precise measurements of UT angle $\phi_1(\beta)$ [1,2] have focussed attention on $|V_{ub}|$, because it determines the side of the UT that is opposite ϕ_1, it directly tests the Kobayashi-Maskawa mechanism [3] for CP violation within the SM.

To date, inclusive measurements of $|V_{ub}|$ have been reported by experiments operating on the $\Upsilon(4S)$ resonance, namely CLEO [4,5,6], ARGUS [7], BaBar [8] and Belle [9], and by LEP experiments operating on the Z resonance, namely L3 [10], ALEPH [11], DELPHI [12] and OPAL [13].

The value of $|V_{ub}|$ can be extracted from the measured rate of charmless semileptonic B-meson decays $B \to X_u e\nu_e$ in a kinematic region that has to be chosen to minimise the impact of the large background from the charmed semileptonic B-meson decays $B \to X_c e\nu_e$. One such region is at the endpoint of the lepton momentum spectrum: in the rest frame of the decaying B meson, leptons from $B \to X_c e\nu_e$ decays attain a maximum momentum of 2.31 GeV/c while for $B \to X_u e\nu_e$ decays the maximum is 2.64 GeV/c.

In this paper we report measurements of partial branching fractions to inclusive charmless semileptonic B-meson decays from the yield of electrons and positrons in six overlapping momentum intervals. The intervals have lower

[1] on leave from Nova Gorica Polytechnic, Nova Gorica, Slovenia

limits commencing at 1.9 GeV/c through 2.4 GeV/c incremented in steps of 0.1 GeV/c and a common upper limit of 2.6 GeV/c, as measured in the centre of mass (CM) [2] frame.

We use two methods to extract $|V_{ub}|$, one that has been standard practice [14] (DFN), and one that has been recently developed [15,16,17,18,19](BLNP). The DFN method involves extrapolation from a partial to a full branching fraction using the DeFazio-Neubert prescription with given shape function parameters [20] followed by a routine to translate the full branching fraction to $|V_{ub}|$ [14]. The BLNP method in contrast to the DFN method provides a more systematic treatment of shape function effects by incorporating all known contributions, includes power corrections, uses an improved perturbative treatment and directly relates the $B \to X_u e \nu_e$ partial rate to $|V_{ub}|$. For both methods we use values for the parameters of the shape function that were determined using the $B \to X_s \gamma$ photon energy spectrum measured by Belle [21] [3]. In the case of DFN the procedure and measurements are given in Ref. [24]. The same procedure was updated with predicted shapes of the $B \to X_s \gamma$ photon energy distributions from Ref [25] to yield values of shape function parameters relevant to the BLNP method. The latter are equivalent to HQET parameters in the shape function scheme [19].

2 Detector and Data Sample

The results reported here are based on data collected with the Belle detector at the KEKB asymmetric energy e^+e^- collider [26]. The Belle detector is a large-solid-angle magnetic spectrometer that consists of a three-layer silicon vertex detector (SVD), a 50-layer central drift chamber (CDC), an array of aerogel threshold Čerenkov counters (ACC), a barrel-like arrangement of time-of-flight scintillation counters (TOF), and an electromagnetic calorimeter comprised of CsI(Tl) crystals (ECL) located inside a superconducting solenoid coil that provides a 1.5 T magnetic field. An iron flux-return located outside of the coil is instrumented to detect K_L^0 mesons and to identify muons (KLM). The detector is described in detail elsewhere [27]. We use 27.0 fb^{-1} and 8.8 fb^{-1} integrated luminosity samples taken at (ON) and 60 MeV below (OFF) the $\Upsilon(4S)$ resonance energy, respectively. The ON sample consists of 29.4 million $B\overline{B}$ events. Unless explicitly stated otherwise, all variables are calculated in the CM frame.

[2] The rest frame of the $\Upsilon(4S)$ is equivalent to the centre of mass frame.

[3] The use of the photon energy spectrum from inclusive radiative B-meson decays in determining the b-quark shape function or distribution function was first discussed by Bigi *et* al [22] and Neubert [23].

3 Data Analysis

The procedure for this analysis largely follows that of CLEO [6], and consists of examining the spectrum of electron candidates with momentum in the range $1.5-3.5$ GeV/c, which includes both signal and sideband regions. We initially chose and optimised our selection criteria for the momentum region, $2.2-2.6$ GeV/c. For ease of explanation we discuss the experimental procedure for this momentum interval and later describe the slight differences in the signal extraction for other momentum intervals.

In the CM frame the kinematic endpoint for decays of the type $B \to X_c e\nu_e$, including the non-zero B momentum and detector effects, is 2.4 GeV/c. The $B \to X_u e\nu_e$ signal is extracted in the momentum region $2.2-2.6$ GeV/c (HI), while a lower range, from $1.5-2.2$ GeV/c (LO), is examined to evaluate the contribution from $B \to X_c e\nu$, which is then extrapolated to the HI region.

The uncertainty on the fraction of $B \to X_u e\nu$ within the HI region is a major source of systematic error for the determination of the branching fraction and $|V_{ub}|$. For choosing and optimising selection criteria we use a sample of events containing $B \to X_u e\nu_e$ decays, generated via Monte Carlo simulation and based on a model described in Ref. [28] (ISGW2), which predicts the form factors and branching fractions of the many exclusive charmless semileptonic B-meson decay channels that form the sample. We also generate samples based on an inclusive $B \to X_u e\nu_e$ model, according to the prescription of DeFazio and Neubert [20], with shape function (SF) parameters that correspond to the residual B-meson mass [4] and the average momentum squared of the b-quark inside the B-meson set to $\Lambda^{\rm SF} = 0.659$ GeV/c^2 and $-\lambda_1^{\rm SF} = 0.400\,{\rm GeV}^2/c^2$, respectively. These values were determined from the photon energy spectrum in $B \to X_s\gamma$ decays measured by Belle [24]. To examine the extent to which our results may vary due to uncertainties in $\Lambda^{\rm SF}$ and $\lambda^{\rm SF}$, we also generate four samples with parameters that define the long and short axes of the $\Delta\chi^2 = 1$ contour in the $(\frac{\Lambda^{\rm SF}}{{\rm GeV}/c^2}, \frac{\lambda_1^{\rm SF}}{{\rm GeV}^2/c^2})$ plane, corresponding to $(0.614, -0.231)$, $(0.736, -0.714)$, $(0.719, -0.462)$ and $(0.635, -0.483)$.

3.1 Event Selection

To select hadronic events we require the multiplicity of tracks to be greater than four and the primary event vertex to be within 1.5 cm radially and 3.5 cm longitudinally from the detector origin. We make further requirements based

[4] $\overline{\Lambda^{\rm SF}} = M_B - m_b$;
where m_b and M_B are the masses of the b-quark and B-meson, respectively.

on quantities calculated in the CM frame – that the sum of cluster energies in the ECL satisfies $0.18\sqrt{s} < E_{\rm ECL} < 0.80\sqrt{s}$ where $\sqrt{s}$ is the CM collision energy, that the visible energy $E_{\rm vis}$ be at least $0.50\sqrt{s}$, that the absolute sum of longitudinal track and photon momenta be less than $0.30\sqrt{s}$, that the heavy jet mass be either at least $0.25 \times E_{\rm vis}$ or greater than 1.8 GeV/c^2, and that the average cluster energy be less than 1 GeV. We also require that the ratio R_2 of the second to the zeroth Fox-Wolfram moment [29] be less than 0.5.

3.2 Electron spectrum

Charged tracks are reconstructed from hits in the SVD and the CDC. Tracks are required to pass within a short distance from the interaction point (IP) of the e^+e^- collision, where the B-meson decays promptly. For improved data and MC agreement, tracks must be within the acceptance of the barrel part of the ECL; $-0.63 < \cos\theta_{\rm lab} < 0.85$, where $\theta_{\rm lab}$ is the polar angle measured in the laboratory frame with respect to the direction opposite to that of the positron beam. Tracks are identified as electrons on the basis of a matching energy cluster in the ECL, and, subsequently, upon the ratio of ECL-measured energy to CDC-measured track momentum, transverse shower shape in the ECL, ionisation energy loss in the CDC, and the ACC light yield [30]. Given the track requirements, electrons with momenta in the range $1.5 - 2.6$ GeV/c are positively identified with a probability of $(94.0 \pm 1.5)\%$ while pions are misidentified as electrons with a probability of $(0.13 \pm 0.01)\%$, as measured using samples of reconstructed $J/\psi \to e^+e^-$ and $K^0_S \to \pi^+\pi^-$ decays, respectively.

To reduce the contribution of electrons from J/ψ and $\psi(2S)$ decays and photon conversions, our candidate electrons are paired with oppositely charged tracks identified as electrons in the event and rejected if their mass falls within either J/ψ, $\psi(2S)$ or γ mass windows, defined as $[3.025, 3.125]\,{\rm GeV}/c^2$, $[3.614, 3.714]\,{\rm GeV}/c^2$ and $[0, 0.1]\,{\rm GeV}/c^2$, respectively. The photon conversion veto has the additional effect of removing electrons from π^0 Dalitz decays. The yields of candidates that do not pass the J/ψ veto requirement are compared in data and MC to determine a normalisation factor for MC-estimated backgrounds, which are described below.

Since the dynamics of the hadronic part of $B \to X_u e\nu_e$ is not well established, it is important that selection requirements retain acceptance over a wide range of $q^2 \equiv (p_e + p_\nu)^2$ (dilepton invariant mass squared) in order to minimise model dependence. Additional event requirements are designed to reduce contributions from continuum ($e^+e^- \to q\bar{q}$ where $q = u, d, s, c$) and QED-related processes (including two photon and tau-pair events) without introducing a q^2 bias. A set of "energy flow" variables is formed by grouping

detected particles in bins of 0.05 in $\cos\theta$, where θ is the particle angle with respect to the candidate electron, and taking the energy sum in each bin. The energy flow in the backward direction $-1.00 < \cos\theta < -0.95$ is not used, as it is found to disproportionately reduce the acceptance in the low q^2 region. A Fisher discriminant, denoted $\mathcal{F}_{\rm FLOW}$, is constructed from the remaining energy flow variables with coefficients chosen to best separate signal from continuum events. We also make use of a b-quark rare decay tag variable, denoted $\mathcal{K}$, and calculated as

$$\mathcal{K} = Q(e)\left(N(K^+) - N(K^-)\right), \tag{1}$$

where $Q(e)$ is the charge of the candidate electron, and $N(K^\pm)$ are the number of tracks identified as positively and negatively charged kaons in an event, respectively. $\mathcal{K}$ exploits the presence of lepton-kaon charge correlations evident in $B\overline{B}$ events wherein one B-meson decays via a $b \to ue\nu_e$ transition whilst the other B-meson decays typically via $\overline{b} \to \overline{c} \to \overline{s}$ transitions, thereby resulting in, on average, a net strangeness or kaon charge that is correlated to the charge of our candidate electron. The correlation does not exist in continuum events nor in $B\overline{B}$ events that do not involve the $b \to ue\nu_e$ transition. Charged tracks are identified as kaons by utilising specific ionisation energy loss measurements made with the CDC, light yield readings from the ACC, and time of flight information from the TOF. The average kaon identification efficiency and fake rate in the momentum range 0.5–4.0 GeV/c, as measured in the laboratory frame, are $(88.0 \pm 0.1)\%$ and $(8.5 \pm 0.1)\%$, respectively.

To preserve signal efficiency, the selection requirements on $\mathcal{F}_{\rm FLOW}$ are chosen differently for three cases of $\mathcal{K}$: $\mathcal{K} > 0$; $\mathcal{K} = 0$; and $\mathcal{K} < 0$. The cut values are chosen to optimise the figure of merit $S/\sqrt{S+B}$, where S and B reflect the signal and continuum background expectation, respectively, as estimated from MC events, assuming the branching fraction measured by CLEO [6]. The $\mathcal{K}$ dependent cuts on $\mathcal{F}_{\rm FLOW}$ reduce continuum backgrounds by 97% while retaining 33% of the $B \to X_u e\nu_e$ signal.

To further suppress QED-related continuum backgrounds, the cosine of the angle between the thrust axis of the event and the e^- direction $\cos\theta_{thr}$, is required to be less than 0.75. Crucially, the thrust axis calculation includes the missing momentum as a component. Missing momentum is calculated as the difference between the momentum of the beams and the sum of the observed track and cluster momenta. Placing a constraint on $\cos\theta_{thr}$ was found to bias the q^2 distribution in signal events less than a constraint imposed on the direction of missing momentum, which has been previously used by CLEO [6]. The requirement on $\cos\theta_{thr}$ reduces QED-related continuum backgrounds by 50% with a signal inefficiency of 10%.

The acceptance of the selection requirements as a function of generated q^2 for

events containing electrons in the momentum interval $2.2 - 2.6$ GeV/c from $B \to X_u e \nu_e$ decay is shown in Figure 1.

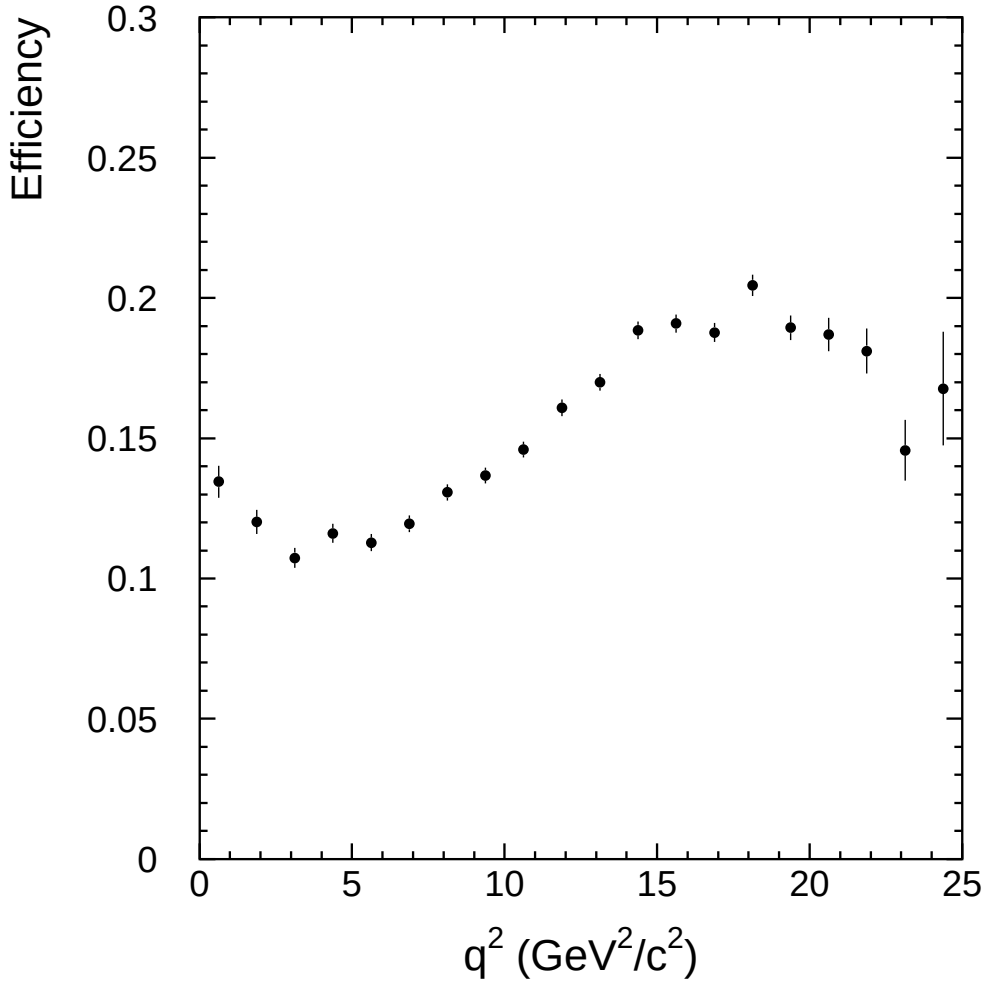

Fig. 1. Acceptance of the selection requirements as a function of generated q^2 for events containing electrons in the region 2.2-2.6 GeV/c from $B \to X_u e \nu_e$ decay.

3.3 Backgrounds

Sources of background for $B \to X_u e \nu_e$ include continuum events, hadrons misidentified as electrons ("fakes"), decays $B \to X_c e \nu_e$, and various secondary decays of B-mesons. We describe below our evaluation of each as well as our procedures for evaluating the associated contributions to the systematic uncertainty.

The continuum contribution is evaluated using the OFF data set. To account for the small difference in the momentum spectra due to the beam energy

difference (0.6%), the electron momenta in OFF data are scaled by the ratio of ON to OFF CM energies. The yields in OFF data are then scaled by the factor $\alpha = 3.005 \pm 0.015$, determined by the ON to OFF ratio of Bhabha event yields in the barrel ECL. As a check of this procedure, we measure the yields in the momentum range $2.8 - 3.5$ GeV/c, above the kinematic maximum for $B\overline{B}$ events. The resulting signal of 85 ± 93 electron candidates is consistent with zero, as expected. We assign systematic uncertainties based on a MC study of the detector response to Bhabha events (0.4%), and the discrepancy with α as calculated, similarly, with dimuon events (0.2%).

The remaining contributions to background are from $B\overline{B}$ events and are estimated using a large Monte Carlo simulated sample of generic $B\overline{B}$ events [31] that contains roughly three and a half times the number of $B\overline{B}$ events in the ON sample. The MC yield due to fakes from charged pions is corrected for the difference in fake efficiency measured by data and MC samples of $K^0_S \to \pi^+\pi^-$ decays. The error on the correction ($\sim 30\%$) is assigned as the systematic uncertainty on the yield from pions. Additional minor contributions from kaons, protons and muons to the overall fakes yield are conservatively assigned systematic uncertainties of 100%.

Of the real electrons, those not from primary $B \to X_c e \nu_e$, secondary backgrounds, are estimated using the Monte Carlo simulated generic $B\overline{B}$ event sample with electronic branching fractions of D^0, D^+, J/ψ, $\psi(2S)$, D_s and τ assigned according to the current world averages [32]. To avoid any bias from a possible mis-modelling of data in MC we use the vetoed J/ψ sample to measure the normalisation factor for both fake and secondary background MC yields. This factor is calculated from a fit of the MC-simulated momentum spectrum of vetoed electron candidates from J/ψ in B-meson decays to the equivalent spectrum obtained from the data. This sample is statistically independent of the final event sample, and, moreover, may not contain neutrinos from primary B-meson decays, which is the case for events providing fake and secondary backgrounds. Contributions from secondary electrons are assigned systematic errors based on the electronic branching fraction uncertainties and the difference between the MC normalisation calculated as described above and that according to the number of $\Upsilon(4S)$ events (6%). Overall, the latter uncertainty has a less than 0.5% effect on the eventual signal yield.

The spectrum from $B \to X_c e \nu_e$ is modelled using three components: $X_c = D$ (HQET [33]); D^* (HQET [33]); and higher resonance charm meson states D^{**} (ISGW2 [28]). To improve the agreement with data, we re-weight the D and D^* components according to q^2 in order to match spectra generated with world average values of form factors [32]. The ratio of D to D^* branching fractions is fixed according to their world average measurements [32]. The proportion of the $(D+D^*)$ component with respect to the D^{**} component is determined from

a binned maximum likelihood fit [34] of the ON data in the LO region [5], where the $B \to X_u e\nu_e$ component is modelled using the inclusive model described earlier and fixed such that $\mathcal{B}(B \to X_u e\nu_e) = (0.25 \pm 0.02)\%$ [14]. For the D^{**} sub-components, D_1 and D_2^* we set $\frac{\mathcal{B}(B\to D_1 e\nu_e)+\mathcal{B}(B\to D_2^* e\nu_e)}{\mathcal{B}(B\to D^{**} e\nu_e)} = 0.35 \pm 0.23$, which has been determined by averaging maximum and minimum assessments of their respective world average branching fractions [32]. Semileptonic spectra are also re-weighted to include the effect of QED radiative corrections as calculated with the PHOTOS algorithm [35]. It has been observed that the KEKB collision energy has variations of $\mathcal{O}(1\,\mathrm{MeV})$ over time and that this results in a measurable variation of the B-meson momentum over the running period of our ON data sample. As our Monte Carlo generator assumes a fixed energy, we apply a shift to the reconstructed momentum in the MC to correct for the difference. The correction depends on the beam energy measurement in the same run period as our ON data set, which is made using a fully reconstructed B-meson decay sample. All spectra for backgrounds other than $B \to X_c e\nu_e$ are derived from the generic $B\overline{B}$ MC sample and handled in the same manner as for the HI region. The goodness-of-fit as estimated by the χ^2/ndf gives 17.8/13. We use this fit result to not only determine the $B \to X_c e\nu_e$ background level in the HI region ($2.2 - 2.6$ GeV/c), but also simultaneously in the signal regions defined as $2.3 - 2.6$ GeV/c and $2.4 - 2.6$ GeV/c.

The same procedure as described above is repeated for three additional HI regions $1.9 - 2.6$ GeV/c, $2.0 - 2.6$ GeV/c, and $2.1 - 2.6$ GeV/c. In each case the LO region is adjusted such that its upper bound equals the lower bound of the HI region, giving respective LO regions of: $1.5{-}1.9$ GeV/c; $1.5{-}2.0$ GeV/c; and $1.5{-}2.1$ GeV/c. The χ^2/ndf for fits in these LO regions are: 6.8/7; 11.9/9; and 13.9/11, respectively.

The systematic error on our measurement due to the uncertainty in the $B \to X_c e\nu_e$ shape and relative normalisations is estimated by varying the parameters fixed in the fit by their individual uncertainties, as described above. The maximum deviation observed from either an upward or downward variation is assigned as the systematic error. We also calculate uncertainties for cases of: no QED radiative correction; an ISGW2 modelled $B \to X_u e\nu_e$ spectrum shape [28]; and the inclusion of a non-resonant $B \to D^{(*)}\pi e\nu_e$ (Goity and Roberts [36]) decay component in the fit. CLEO included the $B \to D^{(*)}\pi e\nu_e$ component in their standard fit [6], but in our case, the shape of its momentum spectrum bears too close a resemblance to that of the $B \to D^{**} e\nu_e$ component. If both $D^{(*)}\pi$ and D^{**} components are included in the fit the D^{**} component floats to zero. This is clearly contrary to observation, given the measured inclusive branching fraction $\mathcal{B}(B \to D^{**} e\nu) = (2.70 \pm 0.70)\%$ [32].

[5] The sum of the yields of the components in the fit is constrained to equal the ON data yield.

The systematic that has the greatest effect on the X_c background estimation in the HI region is the uncertainty on the D^* form factor, which has been obtained by varying the form factor slope parameter ρ^2 within its uncertainty. The net systematic uncertainty is calculated as a sum in quadrature of the individual systematic uncertainties. Table 1 lists the electron candidate yields in ON data, the estimated background contributions and the subsequent extracted signal for the six overlapping momentum intervals.

Table 1
The $B \to X_u e\nu_e$ endpoint and background yields in six momentum intervals, where the first error is statistical and the second is systematic.

$p_{\rm CM}$ (GeV/c)	$2.4 - 2.6$	$2.3 - 2.6$	$2.2 - 2.6$
$N_{\rm ON}$	1741	3534	8854
$\alpha N_{\rm OFF}$	$1166 \pm 59 \pm 5$	$1878 \pm 75 \pm 8$	$2743 \pm 91 \pm 11$
Fakes	$12 \pm 2 \pm 4$	$43 \pm 4 \pm 14$	$85 \pm 5 \pm 28$
$N_{B\to J/\psi\to e}$	$40 \pm 3 \pm 4$	$94 \pm 5 \pm 8$	$191 \pm 7 \pm 17$
$N_{B\to X\to e}$	$8 \pm 1 \pm 1$	$23 \pm 2 \pm 2$	$53 \pm 4 \pm 4$
$N_{B\to X_c e\nu_e}$	$4 \pm 1 \pm 0$	$345 \pm 11 \pm 23$	$3658 \pm 36 \pm 151$
$N_{B\to X_u e\nu_e}$	$512 \pm 73 \pm 7$	$1152 \pm 97 \pm 29$	$2124 \pm 136 \pm 155$

$p_{\rm CM}$ (GeV/c)	$2.1 - 2.6$	$2.0 - 2.6$	$1.9 - 2.6$
$N_{\rm ON}$	23617	54566	104472
$\alpha N_{\rm OFF}$	$3738 \pm 106 \pm 15$	$4900 \pm 121 \pm 20$	$6234 \pm 137 \pm 25$
Fakes	$93 \pm 6 \pm 34$	$131 \pm 7 \pm 40$	$143 \pm 9 \pm 47$
$N_{B\to J/\psi\to e}$	$336 \pm 9 \pm 29$	$562 \pm 12 \pm 49$	$880 \pm 15 \pm 77$
$N_{B\to X\to e}$	$127 \pm 5 \pm 10$	$263 \pm 8 \pm 22$	$553 \pm 11 \pm 48$
$N_{B\to X_c e\nu_e}$	$15494 \pm 73 \pm 437$	$42769 \pm 123 \pm 970$	$87705 \pm 180 \pm 1550$
$N_{B\to X_u e\nu_e}$	$3830 \pm 201 \pm 439$	$5941 \pm 291 \pm 972$	$8957 \pm 395 \pm 1553$

4 Extraction of the partial branching fraction

The inclusive partial branching fraction is found using

$$\Delta\mathcal{B} = \frac{N(B \to X_u e\nu)}{2N_{B\overline{B}}\epsilon_{\rm MC}} \tag{2}$$

where $N_{B\overline{B}} = (29.4 \pm 0.4) \times 10^6$ and the overall selection efficiency is $\epsilon_{\rm MC}$. The systematic uncertainty on the efficiency includes effects from tracking, electron identification, event selection, or model criteria:

- The uncertainty on the track finding for our electron candidates is studied using the MC simulated track embedding method. Care is taken to consider all known sources of uncertainty in the MC simulation: magnetic field effects; CDC wire hit inefficiency; uncertainties in the material budget of the SVD and CDC; and drift time resolution effects in the CDC. The ratio of data to MC single track reconstruction efficiency is consistent with unity at the 1% level. Accordingly, this uncertainty is assigned as the systematic error on the efficiency due to tracking;
- The uncertainty in electron identification (ID) efficiency is measured using inclusive J/ψ events (The method implemented is similar to that described in Ref. [30]). The study involves reconstructing $J/\psi \to e^+e^-$ decays with both tracks satisfying the same track requirements as those of the electron candidates considered for this analysis. We find excellent agreement of the MC simulation with data at the level of 2% and subsequently assign this as the systematic uncertainty on electron identification;
- The effect of the main event selection criteria, namely those of $\mathcal{K}$ dependent $\mathcal{F}_{\rm FLOW}$ and $\cos\theta_{thr}$ cuts, is assessed in two control samples. We fully reconstruct $B^+ \to \overline{D}^0(\to K^+\pi^-)\rho^+(\to \pi^+\pi^0)$ decays. Here the kaon, disregarding particle identification, is assigned as the electron candidate, whilst the pion is regarded as the neutrino. In comparison to $B \to X_u e\nu_e$, the mass of the D meson fixes $q^2 = m_D^2$. The data to MC ratio of the selection efficiency is calculated as a function of CM momentum in the range $1.5 - 2.6$ GeV/c, in bins of 0.05 GeV/c; the best fit is achieved with a constant, which is found to be consistent with unity within 2% uncertainty. We also fully reconstruct $J/\psi \to e^+e^-$ decays and subtract off backgrounds to yield $B \to J/\psi X$ decays. We assign the highest momentum electron from the J/ψ decay to be the electron candidate. The remaining electron is regarded as the neutrino. The mass of the J/ψ-meson fixes $q^2 = m_{J/\psi}^2$. The selection efficiency in this sample was measured as described above, and the best fit, which was also achieved with a constant, found data and MC agree to within 3% uncertainty. Accordingly an overall uncertainty of 4% is assigned as the systematic error due to event selection;
- Model dependence is assessed using the four inclusive samples described above. The maximum shift in selection efficiency is assigned as the systematic uncertainty due to model dependence, and is dependent upon the particular HI region. It varies from 1.7% to 3.4% as the lower momentum limit is increased.

The efficiencies for selecting electrons from $B \to X_u e\nu_e$ decays after all selection criteria have been applied are given in Table 2. Our total efficiency decreases as the lower limit of the electron momentum interval increases, an

effect due mostly to the momentum dependence of the $\mathcal{K}$ dependent $\mathcal{F}_{\rm FLOW}$ cut.

Figure 2(a) shows the ON and scaled OFF momentum spectra along with the total background. Figure 2(b) shows the ON spectrum after background subtraction and efficiency correction, revealing the contribution of $B \to X_u e\nu_e$. The shape prescribed by the inclusive model described earlier, with final state radiation, is also shown. The partial branching fractions for each momentum interval are given in Table 2; as the lower momentum limit is decreased the uncertainty comes to be dominated, as expected, by the uncertainty in the $B \to X_c e\nu_e$ background subtraction. Our partial branching fraction measurements are consistent with those of CLEO and have overall reduced uncertainties [6].

5 Extraction of $|V_{ub}|$

5.1 DFN method

The value of $|V_{ub}|$ is extracted using the formula given in Ref. [14]:

$$|V_{ub}| = 0.00424 \sqrt{\frac{\mathcal{B}(B \to X_u e\nu_e)}{0.002} \frac{1.604 \text{ ps}}{\tau_B}} \times (1.0 \pm 0.028_{\lambda_{1,2}} \pm 0.039_{m_b}), \quad (3)$$

which is an updated version of the expression given in Ref. [32], and includes the latest measurements of the heavy-quark expansion parameters [37]. We average the current world average neutral and charged B-meson lifetimes to obtain $\tau_B = 1.604 \pm 0.011$ ps [32]. To obtain the full inclusive rates for charmless semileptonic B-meson decay from our partial branching fractions, we must determine the spectral fractions f_u and the spectral distortion due to final state radiation loss $\delta_{\rm RAD}$ such that

$$\mathcal{B}(B \to X_u e\nu_e) = \frac{\Delta\mathcal{B}(B \to X_u e\nu_e)}{f_u}(1 + \delta_{\rm RAD}). \quad (4)$$

The value of $\delta_{\rm RAD}$ is calculated from a comparison of MC signal events generated with and without the PHOTOS algorithm implemented. It has been the convention to assign a 10% systematic uncertainty on the correction based on studies that compare the PHOTOS performance with next-to-leading order calculations in $B \to De\nu_e$ decays [38], since the study has yet to be extended to $B \to X_u e\nu_e$ decays, we assign a larger uncertainty, equivalent to a third of

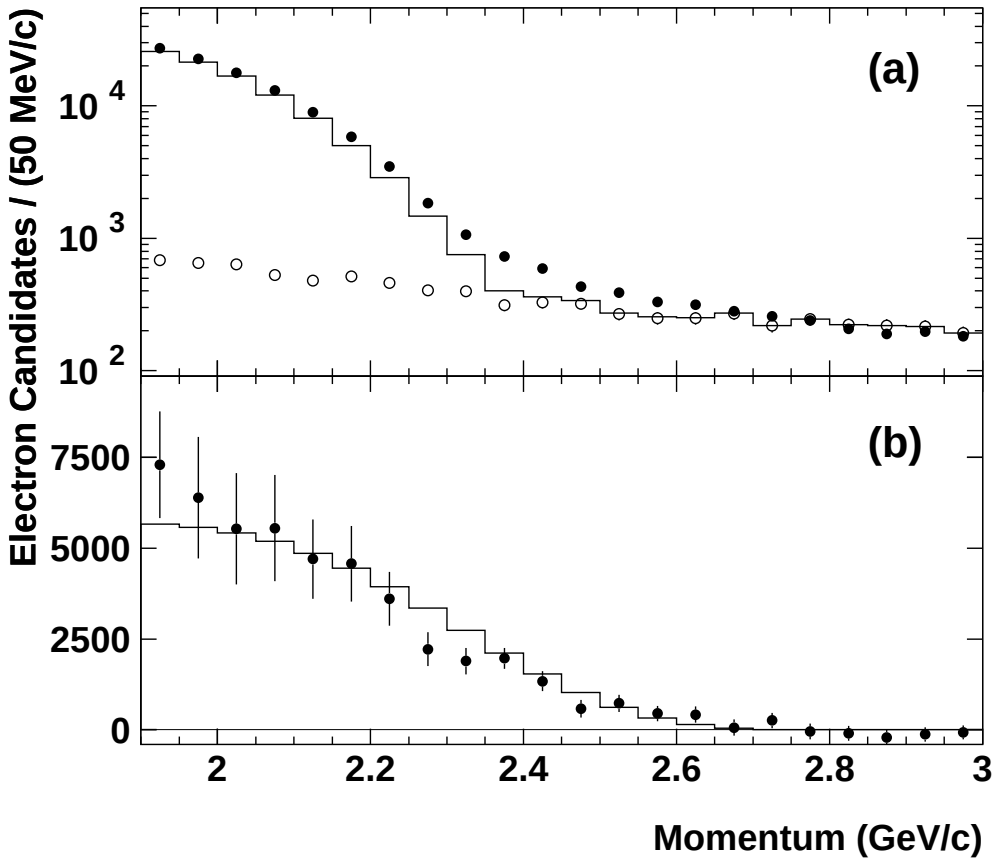

Fig. 2. The electron momentum spectrum in the $\Upsilon(4S)$ rest frame: (a) ON data (filled circles), scaled OFF data (open circles), sum of scaled OFF data and estimated $B\overline{B}$ backgrounds (histogram). (b) ON data after subtraction of backgrounds and correction for efficiency (filled circles) and model spectrum of $B \to X_u e\nu_e$ decays with final state radiation (histogram, normalised to the data yield in the $1.9 - 2.6\,\mathrm{GeV}/c$ momentum range).

the size of the effect. The correction factors for each HI region are given in Table 2.

The values of f_u for the different momentum intervals are determined with the DeFazio-Neubert prescription, using three different forms of the shape function with the parameters, Λ^{SF} and λ_1^{SF}, determined from fits to the Belle measured photon energy spectrum in $B \to X_s\gamma$ decays [21,24]. The resultant values of f_u are given in Table 2, they range from $3 - 32\%$ as the lower momentum limit is decreased. The statistical uncertainty, averaged over each shape function form, is determined from the half-difference of maximum and

Table 2
Branching fractions and extraction of $|V_{ub}|$(DFN method). The reconstruction efficiency, $\epsilon_{\rm MC}$, as calculated from Monte Carlo. The partial branching fractions, $\Delta\mathcal{B}_u(p)$, where the errors are from statistics and experimental systematics, respectively. The lepton momentum spectral fractions, f_u, where the first error is the combined statistical and systematic uncertainty, and the second error is the theoretical uncertainty in extracting shape function parameters from $B \to X_s\gamma$ decays and applying this knowledge to $B \to X_u l\nu_l$ decays. The correction due to the final state radiation loss is denoted $\delta_{\rm RAD}$. The full branching fractions, $\mathcal{B}(B \to X_u l\nu_l)$, where the first error is due to experimental uncertainty and the second is from f_u. The extracted values of $|V_{ub}|$: the first error is experimental; the second error is from f_u, combined statistical and systematic; the third error is from f_u theory; and the last is from the application of the $|V_{ub}|$ formula given in Eqn 3.

$p_{\rm CM}\,({\rm GeV}/c)$	$\epsilon_{\rm MC}(\%)$	$\Delta\mathcal{B}_u(p)(10^{-4})$	f_u
$1.9-2.6$	18.0 ± 0.9	$8.47\pm0.37\pm1.53$	$0.321\pm0.022\pm0.041$
$2.0-2.6$	17.6 ± 0.9	$5.74\pm0.28\pm0.98$	$0.246\pm0.020\pm0.042$
$2.1-2.6$	17.2 ± 0.9	$3.78\pm0.20\pm0.48$	$0.173\pm0.017\pm0.040$
$2.2-2.6$	16.6 ± 0.9	$2.17\pm0.14\pm0.20$	$0.109\pm0.013\pm0.034$
$2.3-2.6$	16.5 ± 0.9	$1.18\pm0.10\pm0.07$	$0.058\pm0.010\pm0.025$
$2.4-2.6$	16.2 ± 1.0	$0.53\pm0.07\pm0.03$	$0.025\pm0.006\pm0.014$
$p_{\rm CM}\,({\rm GeV}/c)$	$\delta_{\rm RAD}$	$\mathcal{B}(B \to X_u e\nu_e)(10^{-3})$	$\lvert V_{ub}\rvert(10^{-3})$(DFN)
$1.9-2.6$	0.06 ± 0.02	$2.80\pm0.52\pm0.41$	$5.01\pm0.47\pm0.17\pm0.32\pm0.24$
$2.0-2.6$	0.07 ± 0.02	$2.49\pm0.45\pm0.47$	$4.73\pm0.42\pm0.19\pm0.40\pm0.23$
$2.1-2.6$	0.07 ± 0.02	$2.34\pm0.33\pm0.59$	$4.59\pm0.32\pm0.22\pm0.53\pm0.22$
$2.2-2.6$	0.09 ± 0.03	$2.16\pm0.25\pm0.73$	$4.41\pm0.25\pm0.27\pm0.69\pm0.21$
$2.3-2.6$	0.10 ± 0.03	$2.22\pm0.24\pm1.02$	$4.47\pm0.24\pm0.36\pm0.96\pm0.22$
$2.4-2.6$	0.11 ± 0.04	$2.39\pm0.38\pm1.46$	$4.63\pm0.37\pm0.53\pm1.32\pm0.22$

minimum f_u found on the $\Delta\chi^2 = 1$ contour in $(\Lambda^{\rm SF}, \lambda_1^{\rm SF})$ parameter space. The systematic error stems from variation of the scale used to evaluate the strong coupling $\alpha_s(\mu)$ ($\mu = m_b/2, 2m_b$) and differences among shape function forms. The theoretical uncertainty is obtained by varying the parameters by $\pm20\%$, reflecting the fact that the procedure is correct only to leading order in the HQET expansion that describes the non-perturbative dynamics of B-mesons. Our variation is twice that considered by CLEO ($\pm10\%$). At the time of their evaluation little was known about sub-leading and weak annihilation effects, they have since been predicted to be large [39,40,41] and are better represented by a $\pm20\%$ variation. The resulting full branching fractions and extracted values of $|V_{ub}|$ are given in Table 2. All the uncertainties contributing

to $|V_{ub}|$ are summarised in Table 3 for each momentum interval. As expected, as the lower momentum cutoff is decreased, the uncertainty from f_u that is due to theory, decreases, while the main experimental systematic, the estimation of $B \to X_c e\nu_e$, increases, in line with its background contribution. The best overall precision (13%) on $|V_{ub}|$, based on a sum in quadrature of experimental and theoretical uncertainties, is found for the $1.9 - 2.6$ GeV/c momentum interval with

$$|V_{ub}| = (5.01 \pm 0.47 \pm 0.17 \pm 0.32 \pm 0.24) \times 10^{-3}, \tag{5}$$

where the first error is from experiment, the second and third are due to experiment and theory errors on f_u, respectively, and the last is the uncertainty in applying the $|V_{ub}|$ extraction formula.

Table 3
Uncertainties contributing to the determination of $|V_{ub}|(10^{-3})$ (DFN method). The total error is obtained from a sum in quadrature.

	Momentum Interval (GeV/c)					
Source of Uncertainty	$1.9 - 2.6$	$2.0 - 2.6$	$2.1 - 2.6$	$2.2 - 2.6$	$2.3 - 2.6$	$2.4 - 2.6$
Statistical	0.11	0.12	0.12	0.14	0.19	0.33
$B \to X_c e\nu_e$ background	0.43	0.39	0.26	0.16	0.04	0.00
Other B background	0.03	0.03	0.03	0.04	0.03	0.03
Efficiency-detector	0.12	0.11	0.11	0.10	0.11	0.12
Efficiency-model	0.04	0.04	0.05	0.05	0.05	0.08
$N_{B\overline{B}}$	0.03	0.03	0.03	0.03	0.03	0.03
$\delta_{\rm RAD}$	0.05	0.05	0.05	0.06	0.07	0.08
f_u statistical	0.17	0.19	0.22	0.26	0.35	0.51
f_u systematic	0.04	0.05	0.05	0.06	0.09	0.13
f_u theory	0.32	0.40	0.53	0.69	0.96	1.32
$\|V_{ub}\|$: $m_b^{\rm kin}(1\,{\rm GeV})$, $\lambda_{1,2}$	0.24	0.23	0.22	0.21	0.22	0.22
Total	0.64	0.66	0.69	0.81	1.07	1.48

5.2 BLNP method

In this prescription $|V_{ub}|$ is obtained directly from the partial branching fraction $\Delta\mathcal{B}$, using the formula

$$|V_{ub}| = \sqrt{\frac{\Delta\mathcal{B}(1+\delta_{\rm RAD})}{\tau_B}\frac{1}{R}}, \tag{6}$$

where τ_B and $\delta_{\rm RAD}$ are as the same as described previously, and R is the theoretical prediction of the partial rate of $B \to X_u l\nu$ decay in units of $|V_{ub}|^2 {\rm ps}^{-1}$ for a given momentum region. The implementation of the BLNP method relies on a model for the leading order shape function that is constrained by HQET parameters; the mass and average momentum squared of the b-quark, $m_b({\rm SF})$ and $\mu_\pi^2({\rm SF})$, respectively, as defined in the shape function scheme (SF). They are set to $m_b({\rm SF}) = (4.52 \pm 0.07)\,{\rm GeV}/c^2$ and $\mu_\pi^2({\rm SF}) = (0.27 \pm 0.13)\,{\rm GeV}^2/c^2$, as derived from the measurement procedure that is described in the introduction.

Table 4 gives the R and $|V_{ub}|$ values for the overlapping momentum intervals. The first error on R is the experimental uncertainty on the leading order shape function, which is our own estimation calculated as the half-difference of minimum and maximum R values obtained from a set of shape function parameters which lie on the $\Delta\chi^2 = 1$ contour. The second error on R is a theoretical uncertainty stemming from the variation of the matching scales $\mu_i, \bar{\mu}, \mu_h$, sub-leading shape function models and the weak annihilation effect, where the latter effect is constant (± 1.40) for all momentum intervals [25].

Our most precise value, which has an overall uncertainty of 13% as based on the sum in quadrature of all the uncertainties,

$$|V_{ub}| = (5.08 \pm 0.47 \pm 0.42^{+0.26}_{-0.23}) \times 10^{-3}, \tag{7}$$

is found for the $1.9 - 2.6$ GeV/c momentum interval. When the shape function parameters and consequently R are better determined, $|V_{ub}|$ can be recalculated from the partial branching fraction measurements presented in Table 2.

6 Summary

We have measured the inclusive charmless semileptonic B-meson decay branching ratio in six overlapping momentum intervals that encompass the endpoint

Table 4
Predicted partial rate R for $B \to X_u l \nu_l$ and extracted value of $|V_{ub}|$(BLNP method). The first error in R is the shape function error stemming from the uncertainty in the knowledge of HQET parameters and the second is a theoretical uncertainty stemming from the variation of the matching scales $\mu_i, \bar{\mu}, \mu_h$, subleading shape function models and the weak annihilation effect. The first error in $|V_{ub}|$ is the experimental error, and the remaining errors are those propagated from R, respectively.

$p_{\rm CM}\,({\rm GeV}/c)$	$R\,(\lvert V_{ub}\rvert^2{\rm ps}^{-1})$	$\lvert V_{ub}\rvert\,(10^{-3})$(BLNP)
$1.9-2.6$	$21.69 \pm 3.62^{+2.18}_{-1.98}$	$5.08 \pm 0.47 \pm 0.42^{+0.26}_{-0.23}$
$2.0-2.6$	$16.05 \pm 3.05^{+1.83}_{-1.72}$	$4.87 \pm 0.43 \pm 0.46^{+0.28}_{-0.26}$
$2.1-2.6$	$10.86 \pm 2.51^{+1.61}_{-1.57}$	$4.83 \pm 0.33 \pm 0.56^{+0.36}_{-0.35}$
$2.2-2.6$	$6.46 \pm 1.54^{+1.54}_{-1.53}$	$4.77 \pm 0.26 \pm 0.57^{+0.57}_{-0.56}$
$2.3-2.6$	$3.15 \pm 0.88^{+1.55}_{-1.54}$	$5.07 \pm 0.71 \pm 0.52^{+1.25}_{-1.24}$
$2.4-2.6$	$1.12 \pm 0.39^{+1.48}_{-1.48}$	$5.70 \pm 1.00 \pm 0.67^{+3.77}_{-3.76}$

of the electron momentum spectrum. These included a momentum interval with a minimum lower momentum cutoff of $1.9\,{\rm GeV}/c$, from which the partial branching fraction was measured to be $\Delta\mathcal{B} = (8.47 \pm 0.37 \pm 1.53) \times 10^{-4}$. We have extracted $|V_{ub}|$ using both the DFN and BLNP methods, but we adopt the results of the latter method since it is more advanced. The most precise $|V_{ub}|$ value was extracted from the decay rate in the $1.9-2.6$ GeV/c momentum interval and found to be $|V_{ub}| = (5.08 \pm 0.47 \pm 0.42^{+0.26}_{-0.23}) \times 10^{-3}$. Owing to updated knowledge of background shapes and normalisations, as well as the improvement in the theoretical prediction of the decay rates for $B \to X_u e \nu_e$ and $B \to X_s \gamma$ decays, the precision of the present measurement is better than that of the previous endpoint measurement by CLEO [6]. Although endpoint methods have not been preferred for a precison determination of $|V_{ub}|$ from inclusive decays [42,43], the results presented in this letter for the momentum interval $1.9-2.6\,{\rm GeV}/c$ are competitive in precision with measurements that have utilised the favoured kinematic regions of hadronic mass and dilepton mass squared [8,9]. This competitiveness is due to a minimum lower momentum cutoff of $1.9\,{\rm GeV}/c$. Our results also, independent of the extracted value of $|V_{ub}|$, help to bound theoretical uncertainties that in general are encountered in all $|V_{ub}|$ extractions from inclusive charmless semileptonic B-meson decays, for example, those relating to quark-hadron duality and the weak annihilation effect [44].

The comparison of our result with other experimental measurements of $|V_{ub}|$ [6,8,9] must be made on a consistent basis, that is, the extraction of $|V_{ub}|$ from a partial branching fraction measurement needs to be performed using a common theoretical framework with common inputs.

ACKNOWLEDGEMENTS

We are grateful to Matthias Neubert, Bjorn Lange, Gil Paz and Stefan Bosch for very helpful discussions, correspondences, explanations and for providing us with their theoretical computations implemented in an inclusive generator. We thank the KEKB group for the excellent operation of the accelerator, the KEK cryogenics group for the efficient operation of the solenoid, and the KEK computer group and the National Institute of Informatics for valuable computing and Super-SINET network support. We acknowledge support from the Ministry of Education, Culture, Sports, Science, and Technology of Japan and the Japan Society for the Promotion of Science; the Australian Research Council, the Australian Department of Education, Science and Training, Australian Postgraduate Award and the David Hay Postgraduate Writing-Up Award; the National Science Foundation of China under contract No. 10175071; the Department of Science and Technology of India; the BK21 program of the Ministry of Education of Korea and the CHEP SRC program of the Korea Science and Engineering Foundation; the Polish State Committee for Scientific Research under contract No. 2P03B 01324; the Ministry of Science and Technology of the Russian Federation; the Ministry of Higher Education, Science and Technology of the Republic of Slovenia; the Swiss National Science Foundation; the National Science Council and the Ministry of Education of Taiwan; and the U.S. Department of Energy.

References

[1] K. Abe *et al.* [Belle Collaboration], Phys. Rev. Lett. **87** (2001) 091802.
K. Abe *et al.* [Belle Collaboration], Phys. Rev. D **66** (2002) 032007.
K. Abe *et al.* [Belle Collaboration], Phys. Rev. D **66** (2002) 071102.

[2] B. Aubert *et al.* [BABAR Collaboration], Phys. Rev. Lett. **87** (2001) 091801.
B. Aubert *et al.* [BABAR Collaboration], Phys. Rev. D **66** (2002) 032003.
B. Aubert *et al.* [BABAR Collaboration], Phys. Rev. Lett. **89** (2002) 201802.

[3] M. Kobayashi and T. Maskawa, Prog. Theor. Phys. **49** (1973) 652.

[4] R. Fulton *et al.* [CLEO Collaboration], Phys. Rev. Lett. **64** (1990) 16.

[5] J. Bartelt *et al.* [CLEO Collaboration], Phys. Rev. Lett. **71** (1993) 4111.

[6] A. Bornheim *et al.* [CLEO Collaboration], Phys. Rev. Lett. **88** (2002) 231803.

[7] H. Albrecht *et al.* [ARGUS Collaboration], Phys. Lett. B **234** (1990) 409.

[8] B. Aubert *et al.* [BABAR Collaboration], Phys. Rev. Lett. **92** (2004) 071802.

[9] H. Kakuno *et al.* [BELLE Collaboration], Phys. Rev. Lett. **92** (2004) 101801.

[10] M. Acciarri *et al.* [L3 Collaboration], Phys. Lett. B **436** (1998) 174.

[11] R. Barate *et al.* [ALEPH Collaboration], Eur. Phys. J. C **6** (1999) 555.

[12] P. Abreu *et al.* [DELPHI Collaboration], Phys. Lett. B **478** (2000) 14.

[13] G. Abbiendi *et al.* [OPAL Collaboration], Eur. Phys. J. C **21** (2001) 399.

[14] H. F. A. Group, arXiv:hep-ex/0412073.

[15] S. W. Bosch, B. O. Lange, M. Neubert and G. Paz, Nucl. Phys. B **699** (2004) 335.

[16] M. Neubert, Eur. Phys. J. C **40** (2005) 165.

[17] S. W. Bosch, M. Neubert and G. Paz, JHEP **0411** (2004) 073.

[18] M. Neubert, arXiv:hep-ph/0411027.

[19] M. Neubert, Phys. Lett. B **612** (2005) 13.

[20] F. De Fazio and M. Neubert, JHEP **9906** (1999) 017.

[21] P. Koppenburg *et al.* [Belle Collaboration], Phys. Rev. Lett. **93** (2004) 061803.

[22] I. I. Y. Bigi, M. A. Shifman, N. G. Uraltsev and A. I. Vainshtein, Int. J. Mod. Phys. A **9** (1994) 2467.

[23] M. Neubert, Phys. Rev. D **49** (1994) 4623.

[24] A. Limosani and T. Nozaki [Heavy Flavor Averaging Group], arXiv:hep-ex/0407052.

[25] B. O. Lange, M. Neubert and G. Paz, arXiv:hep-ph/0504071 and private communication with B. O. Lange, M. Neubert and G. Paz.

[26] S. Kurokawa, Nucl. Inst rum. Meth. A **499** (2003) 1., and other papers included in this Volume.

[27] A. Abashian *et al.* [Belle Collaboration], Nucl. Instrum. Meth. A **479** (2002) 117.

[28] D. Scora and N. Isgur, Phys. Rev. D **52** (1995) 2783.

[29] G. C. Fox and S. Wolfram, Phys. Rev. Lett. **41** (1978) 1581.

[30] K. Hanagaki, H. Kakuno, H. Ikeda, T. Iijima and T. Tsukamoto, Nucl. Instrum. Meth. A **485** (2002) 490.

[31] Events are generated with the CLEO QQ generator, see http://www.lns.cornell.edu/public/CLEO/soft/QQ;
the detector response is simulated with GEANT, R. Brun *et al.*, GEANT 3.21 CERN Report DD/EE/84-1, 1984.

[32] S. Eidelman *et al.* [Particle Data Group], Phys. Lett. B **592** (2004) 1.

[33] Form factors measured in J. E. Duboscq *et al.* [CLEO Collaboration], Phys. Rev. Lett. **76** (1996) 3898, are used as input to the Heavy Quark Effective Theory, see, e.g., M. Neubert, Phys. Rept. **245** (1994) 259.

[34] R. J. Barlow and C. Beeston, Comput. Phys. Commun. **77** (1993) 219.

[35] E. Barberio and Z. Was, Comput. Phys. Commun. **79** (1994) 291.

[36] J. L. Goity and W. Roberts, Phys. Rev. D **51** (1995) 3459.

[37] B. Aubert *et al.* [BABAR Collaboration], Phys. Rev. Lett. **93** (2004) 011803.

[38] E. Richter-Was, Z. Phys. C **61** (1994) 323.

[39] A. K. Leibovich, Z. Ligeti and M. B. Wise, Phys. Lett. B **539** (2002) 242.

[40] C. W. Bauer, M. Luke and T. Mannel, Phys. Lett. B **543** (2002) 261.

[41] M. Neubert, Phys. Lett. B **543** (2002) 269.

[42] C. W. Bauer, Z. Ligeti and M. E. Luke, Phys. Rev. D **64** (2001) 113004.

[43] S. W. Bosch, B. O. Lange, M. Neubert and G. Paz, Phys. Rev. Lett. **93** (2004) 221801.

[44] L. Gibbons [CLEO Collaboration], AIP Conf. Proc. **722** (2004) 156.